

# Unfolding collapsed polyelectrolytes in alternating-current electric fields

Pai-Yi Hsiao,<sup>\*a</sup> Yu-Fu Wei<sup>a</sup> and Hsueh-Chia Chang<sup>b</sup>

Received 23rd August 2010, Accepted 20th October 2010

DOI: 10.1039/c0sm00848f

We investigate the unfolding of single polyelectrolyte (PE) chains collapsed by trivalent salt under the action of alternating-current (AC) electric fields through computer simulations and theoretical scaling. The results show that a collapsed chain can be unfolded by an AC field when the field strength exceeds the direct-current (DC) threshold and the frequency is below a critical value, corresponding to the inverse charge relaxation/dissociation time of condensed trivalent counterions at the interface of the collapsed electrolyte. This relaxation time is also shown to be identical to the DC chain fluctuation time, suggesting that the dissociation of condensed polyvalent counterion on the collapsed PE interface controls the polyelectrolyte dipole formation and unfolding dynamics under an AC electric field.

## I. Introduction

To develop new ability to separate and stretch biomolecules, such as nucleic acids and proteins, is very important in molecular biology and medical research for applications in single molecule analysis and DNA sequencing.<sup>1–4</sup> The conventional way to determine the genetic information of a DNA molecule relies on a series of cumbersome operations of subcloning and electrophoretic separation.<sup>5</sup> This current method reads the sequence of DNA fragments a hundred base-pairs at a time, which has become inadequate for individualized genetic studies.<sup>2</sup> To improve the efficiency of sequencing, single-molecule sequencing methods have been developed recently,<sup>2–4</sup> in which the genetic information of individual DNA molecules is scanned in a linear fashion. One of the key problems in these methods concerns the unfolding of DNA molecules to increase the spatial resolution of scanning, as DNA molecules are long polyelectrolyte (PE) chains that usually adopt the coiled conformation in a typical buffer. In the past decade, many techniques have been developed to stretch PE chains, including the utilization of optical tweezers,<sup>6</sup> fluid flows,<sup>7</sup> electric fields,<sup>8–12</sup> and other methods.<sup>13–15</sup> Among these methods, stretching PE chains in electric fields has received considerable attention, as electrokinetics has become a viable microfluidic method for on-chip molecular analysis.<sup>16,17</sup>

DNA electrophoresis is usually performed in a sieving medium, such as a gel or a polymer solution.<sup>18,19</sup> In this case, DNA chains transform cyclically between an extended structure, with one end hooked onto obstacles in the medium, and a coiled structure when released from the obstacles.<sup>20</sup> If an alternating-current (AC) electric field of appropriate frequency is applied instead, the conformation of the chain in a sieving medium can be maintained constantly in an elongated structure.<sup>10,11</sup> In a bulk buffer, coiled DNA chains have been demonstrated to be stretched in a strong direct-current (DC) electric field, through the mechanism of polarization.<sup>8,21</sup> Nevertheless, there is a drawback to this method: a strong DC field leads easily to electrolytic

dissociation of water molecules.<sup>8,22</sup> To avoid this drawback, a short-duration pulse or an AC electric field has been suggested, with the period shorter than the dissociation reaction time. Moreover, the mean displacement of PE chains in an AC field is zero. This feature could be used to trap or to manipulate single DNA molecules in some place to facilitate the detection of the sequence, particularly when it is integrated with a dielectrophoresis trapping mechanism.<sup>17</sup> Experiments have shown that AC electric field can indeed stretch and orient DNA chains in aqueous solutions at low AC frequency and the chain polarization is largely reduced while the frequency is elevated.<sup>23,24</sup> Recently, Wang *et al.* demonstrated that the conformational transition of single PEs possesses a hysteretic nature upon sweeping the frequency of AC electric field.<sup>25</sup>

Without a solid medium to break the symmetry of the coil–stretch transitions, a low-frequency AC field should stretch the DNA repeatedly during every half-cycle, in a manner of a quasi-DC field. However, unlike DC stretching, the polarization and stretching dynamics now become important, as the molecule must be fully stretched within one half period. It is known that multivalent cations have dramatic effects on the properties and structures of DNA molecules in aqueous solutions.<sup>26</sup> Coiled DNA chains can collapse into globule particles while the chain charge is neutralized by the condensed multivalent cations.<sup>26,27</sup> Experiments have shown that a collapsed DNA chain can be unfolded in DC electric fields if the field strength surpasses a threshold.<sup>28</sup> This threshold  $E^*$  depends on the chain length  $N$ , and the dependence has been studied recently by computer simulations.<sup>29–32</sup> The results suggested a power law-like relation  $E^* \sim N^{-\theta}$  and the electrophoretic mobility of chain depends strongly on whether the chain is unfolded or not. These studies provide a solid foundation to separate PE chains by length in free solutions, based upon the drastic mobility change when a chain is unfolded by an applied electric field.<sup>31</sup> Moreover, recent study in protein mass spectrometry showed that AC electrospray ionization (ESI) yields an effective ionization without fragmenting molecules, with higher ionization efficiency than DC ESI.<sup>33</sup> The ionization efficiency is a sensitive function of sample pH and molecular conformation. It is still unclear whether the higher efficiency is due to the increased local pH or the conformational change or both of the two effects.

<sup>a</sup>Department of Engineering and System Science, National Tsing Hua University, Hsinchu, Taiwan, 30013, R.O.C. E-mail: pyhsiao@ess.nthu.edu.tw

<sup>b</sup>Department of Chemical and Biomolecular Engineering, University of Notre Dame, IN, 46556, U.S.A. E-mail: hchang@nd.edu

This present work constitutes a fundamental molecular dynamics study of how an AC field affects the conformation of a PE chain and the condensation of counterions, and how the field strength required to unfold the chain varies with frequency, in order to give deep insight into the complicated behavior of PE solutions in AC fields. The rest of the paper is organized as follows. We describe the model and simulation setup in Sec. II. The results and discussions are presented in Sec. III. The topics include: chain unfolding in AC electric fields (Sec. III.A), simulation snapshots (Sec. III.B), theoretical explanation (Sec. III.C), time evolution of dipole moment and chain unfolding (Sec. III.D), and the study of polarization time and fluctuation time (Sec. III.E). A summary is given in Sec. IV.

## II. Simulation model and setup

Our system contains a single linear chain, modeled by a bead-spring chain model. The chain is composed of  $N$  monomers. Each monomer carries a negative unit charge  $-e$  and dissociates one monovalent counterion into the solution. The bond connection on the chain is modeled by the finitely extensible nonlinear elastic potential

$$U_{\text{FENE}}(b) = -\frac{1}{2}kb_{\text{max}}^2 \ln\left(1 - \frac{b^2}{b_{\text{max}}^2}\right) \quad (1)$$

where  $b$  is the bond length between two neighboring monomers,  $b_{\text{max}}$  the maximum extension, and  $k$  the spring constant. The condensation of the PE chain is induced by adding (3 : 1)-salt into the system. The salt molecules dissociate into trivalent cations (also called “counter-ions”) and monovalent anions (also called “co-ions”) in the solution. All these particles, including monomers, counter-ions, and co-ions, are modeled as Lennard–Jones (LJ) spheres, described by the potential

$$U_{\text{LJ}}(r) = \begin{cases} 4\epsilon_{\text{LJ}}\left[(\sigma/r)^{12} - (\sigma/r)^6 + 1/4\right] & , \text{ for } r \leq \sqrt[6]{2}\sigma \\ 0 & , \text{ for } r > \sqrt[6]{2}\sigma \end{cases} \quad (2)$$

where  $\sigma$  and  $\epsilon_{\text{LJ}}$  represent the diameter and the hardness of the LJ sphere, respectively, and  $r$  is the distance between two particles. Since the interaction between the monomers is purely repulsive, this setup corresponds to a good solvent condition. Particles also interact with each other *via* the Coulomb interaction, which reads as

$$U_{\text{C}}(r) = k_{\text{B}}T \cdot \frac{Z_i Z_j \lambda_{\text{B}}}{r} \quad (3)$$

where  $k_{\text{B}}T$  is the thermal energy and  $Z_i$  is the charge valence of the  $i$ th particle. The Bjerrum length  $\lambda_{\text{B}} = e^2/(4\pi\epsilon_0\epsilon_r k_{\text{B}}T)$  is the distance between two unit charges, at which the electrostatic energy is equal to the thermal energy, where  $\epsilon_0$  is the vacuum permittivity and  $\epsilon_r$  is the relative dielectric constant of solvent. The solvent molecules are not modeled explicitly in the study. However, their effects are incorporated implicitly by the following three ways: (1) dielectric screening of charge by  $\epsilon_r$ , (2) friction force,  $-m_i\zeta_i\dot{\vec{r}}_i$ , due to particle moving through the solvent, (3) stochastic force,  $\vec{\eta}_i(t)$ , owing to thermal collisions of solvent molecules. The equation of motion, also known as the Langevin equation, thus reads as

$$m_i\ddot{\vec{r}}_i = -m_i\zeta_i\dot{\vec{r}}_i + \vec{F}_c + Z_i e E(t)\hat{x} + \vec{\eta}_i \quad (4)$$

where  $m_i$  is the particle mass,  $m_i\zeta_i$  is the friction coefficient, and  $\vec{F}_c = -\partial U/\partial\vec{r}_i$  is the conservative force. In this equation, the temperature  $T$  is controlled by the fluctuation–dissipation theorem:  $\langle\vec{\eta}_i(t)\cdot\vec{\eta}_j(t')\rangle = 6k_{\text{B}}Tm_i\zeta_i\delta_{ij}\delta(t-t')$ . The system is placed in a periodic rectangular box. The AC field  $E(t)$  is a square wave applied in the  $x$ direction. The period of the square wave is  $\Psi$  and the field strength is  $|E|$ . Particle–particle particle–mesh Ewald sum<sup>34</sup> is used to calculate Coulomb interaction.

We simulate aqueous PE solutions at room temperature ( $T = 300$  K) and assume that all the particles have the same mass  $m$  and LJ parameters  $\sigma$  and  $\epsilon_{\text{LJ}}$ . We set  $\epsilon_{\text{LJ}} = 0.8333k_{\text{B}}T$ ,  $k = 5.8333k_{\text{B}}T/\sigma^2$ ,  $b_{\text{max}} = 2\sigma$ ,  $\lambda_{\text{B}} = 3\sigma$ , and  $\zeta_i = 1.0\tau^{-1}$  where  $\tau = \sigma\sqrt{m/(k_{\text{B}}T)}$  is the time unit. Since  $\lambda_{\text{B}}$  is 7.1 Å for water, the length unit  $\sigma$  corresponds to 2.4 Å. The time unit  $\tau$  is about 1.5 ps if  $m$  is taken to be a typical monomer mass of the order 100 g mol<sup>-1</sup>. This set of parameters can be used to model flexible PE chains in water, such as sodium polystyrene sulfonate. The dimension of our simulation box is  $153.6\sigma \times 79.06\sigma \times 79.06\sigma$  and the chain length  $N$  is 96. It yields the monomer concentration  $C_{\text{m}}$  equal to  $0.0001\sigma^{-3}$ , which is about 12 mM in real units. This  $C_{\text{m}}$  describes a dilute PE solution. The salt concentration  $C_{\text{s}}$  is set to the equivalence point  $C_{\text{s}}^* = C_{\text{m}}/3$ . It has been shown that at  $C_{\text{s}} = C_{\text{s}}^*$ , the trivalent counter-ions form complexes with the chain, largely neutralizing the bare chain charge; the chain collapses into a globule structure.<sup>26,27,35,36</sup> The  $\Psi$  and  $|E|$  are varied over a wide range of values to study their effects on the properties of the PE system. The Langevin equation is integrated by the Verlet algorithm with a time step  $\Delta t$  equal to  $0.005\tau$ .<sup>37</sup> A pre-run phase takes about  $10^7$  time steps to bring the system into a stationary state for each ( $\Psi$ ,  $|E|$ )-case, followed by a production-run phase of  $10^8$  time steps to cumulate data for analysis. The hydrodynamic interaction is not included in this work because it is largely screened out under typical electrophoretic conditions.<sup>19,38,39</sup> A recent study clearly demonstrated this point.<sup>40</sup> To simplify the notation, physical quantities in the following text will be reported in a ( $\sigma$ ,  $m$ ,  $k_{\text{B}}T$ ,  $e$ )-unit system if not specially mentioned. For *e.g.*, the strength of electric field will be described in unit  $k_{\text{B}}T/(e\sigma)$ .

## III. Results and discussions

### A. Degree of chain unfolding

We firstly revisited a reference case in which the applied field is a DC electric field. It is the limiting case of an AC field with infinite  $\Psi$ . The degree of chain unfolding  $D_{\text{s}}$ , defined as the ratio of the end-to-end distance  $R_{\text{c}}$  of chain to the contour length  $L_{\text{c}}$ , is shown in Fig. 1(a) against the DC field strength  $E_{\text{dc}}$ .

We can see that  $D_{\text{s}}$  shows a sharp transition, occurred at  $E_{\text{dc}}^* = 0.22$ . Below  $E_{\text{dc}}^*$ , the PE chain stays in a collapsed state, in which condensed trivalent counter-ions tightly bind monomers together, resulting in a chain size similar to the unperturbed size in zero field. The structure of the collapsed chain is a spherical globule. When  $E_{\text{dc}} > E_{\text{dc}}^*$ , the chain unfolds abruptly. The DC field is strong enough to drive the condensed trivalent counter-ions towards one side of the chain globule and even more, strips them off the chain. The chain is hence elongated and aligned in

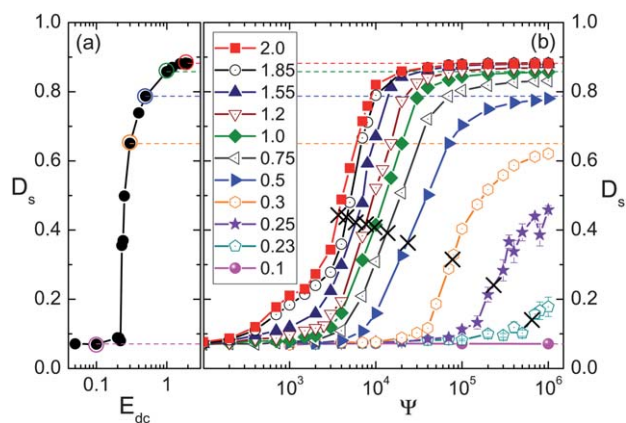


**Fig. 1** (a)  $D_s = R_c/L_c$  in DC fields as a function of  $E_{dc}$ ; (b)  $D_s$  as a function of  $\Psi$  (in unit  $\Delta t$ ) in AC fields of different  $|E|$ . The value of  $|E|$  is indicated in the inset of the figure. The symbol 'X' denotes the inflection point on each corresponding curve. The error bar of data, if not shown, is smaller than the symbol size of data in this paper.

the field direction in the process. The degree of chain unfolding can be as large as 90% of the contour length when  $E_{dc}$  is large enough. The detailed study including the effect of salt concentration and valence on chain unfolding as well as the scaling law for  $E_{dc}^*$  against  $N$  in DC fields can be found in Ref. 31 and 32. An independent simulation done recently by another group<sup>41</sup> also confirms our results.

We then studied the case with AC fields. The degree of chain unfolding is now plotted against the field period  $\Psi$  in Fig. 1(b) for different field strengths  $|E|$ . The results show that  $D_s$  takes the value of zero field, 0.07, over the whole range of  $\Psi$  when  $|E| < E_{dc}^*$ . In this situation, the field strength is too weak to overcome the binding of the condensed trivalent counterions to unfold the chain. When  $|E| > E_{dc}^*$ , chain unfolding can take place and  $D_s$  is a sigmoidal function of  $\Psi$ . When  $\Psi$  is small, the applied field alters very frequently. The duration of a half period of the field, within which the square-wave field acts as a DC one pointing to either  $+x$  or  $-x$  direction, is not long enough either for the chain to complete its conformational change or for the condensed counter-ions to migrate to stable positions. The degree of chain unfolding is thus small. When  $\Psi$  is sufficiently large, the deformation and the polarization of the PE complex can be completed in a half period. The chain is unfolded and the maximal degree of chain unfolding takes a value corresponding to the limiting value in the referenced DC field. In the figure, the limiting value has been indicated as a dashed line. The reduction of the degree of chain unfolding in the region of small  $\Psi$  is in agreement with experiments;<sup>23,24</sup> a recent simulation<sup>41</sup> also demonstrated a consistent behavior. Moreover, we observed that the transition of  $D_s$  is not really sharp but occurs over a range of period  $\Psi$ . In order to characterize this behavior quantitatively, we define the transition point at  $\Psi = \Psi_c$ , which is the inflection point of the  $D_s$  curve. The inflection point has been indicated by a symbol 'X' on each curve in Fig. 1(b). We saw immediately that  $\Psi_c$  depends strongly on  $|E|$  and the value falls in a range from  $(3 \times 10^3)\Delta t$  to  $(7 \times 10^5)\Delta t$ , or equivalently, from 22.5 ps to 5.25 ns. Therefore, the collapsed chain is unfolded when the AC field

frequency is smaller than the order of tera- or giga-hertz. Detailed studies showing that  $\Psi_c$  is directly related to the characteristic time to fully polarize the PE chain will be presented later. Since chain unfolding occurs in a small frequency region, experiments can verify this phenomenon easily, provided that the AC field strength is stronger than  $E_{dc}^*$ . As shown in our previous DC simulations,<sup>31,32</sup>  $E_{dc}^*$  can be largely reduced to a value of a few hundreds volt per cm if a long PE chain of order, for *e.g.*,  $N = 10^6$ , is used. This strength of AC field is accessible by experiments.

## B. Simulation snapshots

In order to have the picture of chain conformation in mind, we show in Fig. 2 the snapshots of PE chain in AC fields with the field strength equal to 0.3.

Three field periods are presented in the panels: (a)  $\Psi = 10^3\Delta t$ , (b)  $\Psi = (8 \times 10^4)\Delta t$ , and (c)  $\Psi = 10^6\Delta t$ , which are, respectively, smaller than, about equal to, and larger than the critical period  $\Psi_c$  (refer to Fig. 1). In each panel, the evolution of chain shape against a field cycle is shown, following the  $t/\Psi$ -axis. We can see that for the case of small period (Fig. 2(a)), the chain is not unfolded in the AC field. It exhibits a globule structure. This is because the acting time in a half-cycle of the AC field is too short for the chain to respond. On the other hand, for the case of large period as shown in Fig. 2(c), the acting time is long enough. The chain is stretched and displays an elongated structure aligned parallel to the field direction. If we look carefully into the snapshots, we can find that the trivalent counter ions are not uniformly condensed on the chain backbone in this case. They follow the field direction and accumulate more on one of the chain ends. This non-uniform distribution results in a chain polarization. When the AC field switches its direction, the

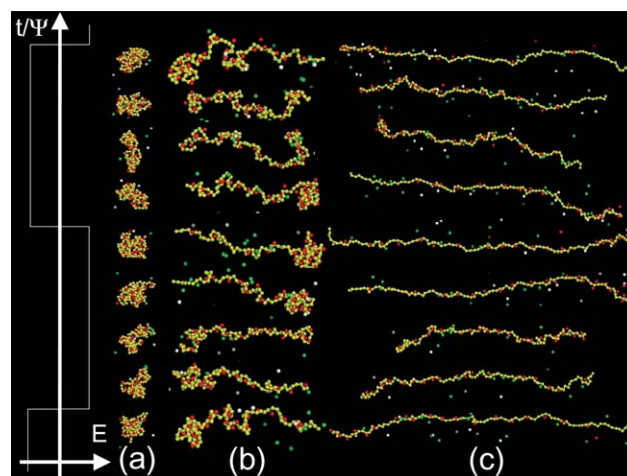


**Fig. 2** Snapshots of PE chain in a cycle of the applied AC field. The field strength  $|E|$  is 0.3 and the field period is (a)  $\Psi = 10^3\Delta t$ , (b)  $\Psi = (8 \times 10^4)\Delta t$ , and (c)  $\Psi = 10^6\Delta t$ . The PE chain is represented by the yellow-colored bead-spring chain. The trivalent counter-ions, the monovalent counter-ions, and the co-ions are represented by the red, green and white beads, respectively. The change of the field direction is indicated on the left side of the figure as a function of field cycle  $t/\Psi$  and the evolution of the chain conformation can be seen in each panel, following the  $t/\Psi$ -axis from bottom to top.

stability of the system is suddenly destroyed and the condensed trivalent ions migrate toward the other chain end. The chain partially shrinks and then regains its size soon after the new stability is established. For the case with the field period close to  $\Psi_c$  (panel (b) of Fig. 2), an astonishing, tadpole-like structure of chain is observed, just before switching of the AC field direction. The head of the tadpole structure is derived from the accumulated trivalent counter-ions binding together with the chain near an end. And the tail is formed by the other side of the chain with less counter-ions condensed on it. Because the chain is partially unfolded, the degree of polarization is smaller than the one in panel (c) (Fig. 2). The change of the AC field direction drives the trivalent counter-ions moving away from the tadpole head toward the tail. As a passage, the head shrinks and the tail grows. Eventually, the new accumulation of the trivalent counterions creates a new head on the other side of the chain. The new tadpole structure thus inverts its heading direction and waits for the next alternating field.

### C. Theory of chain unfolding

The dependence of  $\Psi_c$  on  $|E|$  can be captured by the following charge relaxation theory. We assume that a PE chain is unfolded in an AC field if the polarization energy of the chain complex,  $W_{ac} = \alpha(\omega)|E|^2/2$ , is larger than some critical energy, where  $\omega$  is the field frequency and  $\alpha(\omega)$  is the polarizability. This critical energy can be estimated by  $W_{dc}^* = \alpha(0)E_{dc}^{*2}/2$ , the polarization energy to unfold the chain in the critical DC field  $E_{dc}^*$ . It is known that for a conducting Maxwell–Wagner sphere of arbitrary radius  $R$  in an AC field, the polarizability can be expressed by  $\alpha(\omega) = 4\pi\epsilon_m K(\omega)R^3$  where

$$K(\omega) = \frac{\tilde{\epsilon}_p(\omega) - \tilde{\epsilon}_m(\omega)}{\tilde{\epsilon}_p(\omega) + 2\tilde{\epsilon}_m(\omega)}$$

is the Clausius–Mossotti factor, and  $\tilde{\epsilon}_m$  and  $\tilde{\epsilon}_p$  are the  $\omega$ -dependent complex permittivity of the solvent medium and the PE complex, respectively.<sup>42</sup> This Clausius–Mossotti factor arises due to both the dielectric polarization, resulting from the permittivity difference across the sphere-medium interface, and the space charge accumulation at the interface, derived from the conductivity gradient and the corresponding ion flux discontinuity at that location. While counterion migration occurs across the entire collapsed chain, charge polarization occurs only at the two poles. It involves the dissociation and condensation of the migrating counter-ions presented within a Debye-layer neighborhood of the interface. As a result, the dipole formation time is the usual charge relaxation time at the interface. When the resulting dipole moment aligns parallel to the electric field, a net stretching force is imposed on the chain, corresponding to the polarization energy. The chain is unfolded. The condensed ions hence play a role to the PE chain, similar to the one of the bound surface electrons to a dielectric object. Therefore, the polarization dynamics of the system can be studied by the method of electrical impedance.<sup>42,43</sup>

We model the dielectric response for the PE complex by a resistor–capacitor (RC) circuit in series. The complex permittivity reads as

$$\tilde{\epsilon}_p(\omega) = \frac{\epsilon_p}{1 + i\omega\epsilon_p/\sigma_p} = \frac{\epsilon_p}{1 + i\omega\tau_{rc,p}}$$

The response function for the solvent is modeled by a RC circuit in parallel and the complex permittivity is

$$\tilde{\epsilon}_m(\omega) = \epsilon_m - \frac{i\sigma_m}{\omega} = \epsilon_m \left( 1 - \frac{i}{\omega\tau_{rc,m}} \right)$$

Here  $\epsilon_p$  and  $\sigma_p$  (or  $\epsilon_m$  and  $\sigma_m$ ) are, respectively, the permittivity and the ion conductivity in the PE complex (or in the solvent), and  $\tau_{rc,p} = \epsilon_p/\sigma_p$  and  $\tau_{rc,m} = \epsilon_m/\sigma_m$ . Since the trivalent counterions condensed quite tightly on the chain, the migration of these ions from one side of the PE complex to the other side in an electric field is similar to the electron migration from one plate of a capacitor to the other plate in a voltage source. The ion migration also suffers a resistance force against the applied electric field, a situation which is similar to put a resistor in the circuit. Therefore, we model the PE chain phase by an RC circuit in series. Because the length scale across the phase in the field direction corresponds to both the capacitor gap and the resistor length, the ratio  $\tau_{rc,p}$  is the characteristic time to move the counter-ions from one side of the PE chain to the other side. It corresponds to the RC time of the circuit. In the solvent phase, the ions travel through the whole system. Since the travelling speed is not fast, the medium is a poor conductor for ions. Therefore, we regard the solvent as a leaky dielectric, modeled by an RC circuit in parallel. A similar argument shows that the ratio  $\tau_{rc,m}$  is the RC time for the solvent.

Due to the linear dependence of the conductivity on the ionic strength, the RC time for solvent is also the charge relaxation time of electrolyte, which is equal to the squared Debye screening length divided by the diffusivity of the dominant ions. For the PE phase, this connection is typically not true because the ions conduct through nanoporous structures formed by the twisted chain in the phase, rather than simply through a bulk solution. The RC time for the PE phase is important in determination of the critical frequency. At high frequency, the chain polarization is due to dielectric polarization and the value is small. At low frequency, the “capacitor” is fully charged through conductive polarization by accumulating counter-ions at one pole of the PE globule, producing a large polarization. This polarization can grow even further *via* chain unfolding if the applied electric field is strong.

We assume that the RC time for PE is a constant at the critical points to unfold the chain. Based upon the above assumption for the polarization energy, the critical frequency  $\omega_c$  to unfold a chain is determined by the criterion  $(|E|/E_{dc}^*)^2 = \Re[K(0)]/\Re[K(\omega_c)]$ . Let us consider the case of  $\epsilon_p \approx \epsilon_m$ . We obtain

$$\Xi = \frac{(6\tau_{rc,p}\tau_{rc,m} + 9\tau_{rc,m}^2)\omega_c^2}{4 + (4\tau_{rc,p}^2 - 2\tau_{rc,p}\tau_{rc,m})\omega_c^2 + 4\tau_{rc,p}^2\tau_{rc,m}^2\omega_c^4} \quad (5)$$

where  $\Xi = (|E|/E_{dc}^*)^2 - 1$  is the excess of the squared electric field. When  $\omega_c$  is small, the equation gives  $\Xi \approx \left(\frac{3}{2}\tau_{rc,p}\tau_{rc,m} + \frac{9}{4}\tau_{rc,m}^2\right)\omega_c^2 + O(\omega_c^4)$ , which is a linear function

of  $\omega_c^2$ . The figure  $\Xi$  vs.  $\omega_c^2$  is plotted in Fig. 3 where  $\omega_c$  is calculated by  $2\pi/\Psi_c$ .

The result does show a linear dependence of  $\Xi$  in the region of small  $\omega_c^2$ , which follows the prediction of our theory. Least square fit by eqn (5) using Levenberg–Marquardt algorithm yields  $\tau_{rc,p} = 0.393(8)$  and  $\tau_{rc,m} = 21.2(2)$ . In our simulations, the length unit  $\sigma$  and time unit  $\tau$  are 2.4 Å and 1.5 ps, respectively, while mapped to a real system. Since the trivalent cations condense on the chain and largely neutralize the chain charge, most of the monovalent cations and anions are presented in the bulk solution. Hence, the concentrations of the cations and the anions in the solution are both about 0.0001 ( $\sigma^{-3}$ ), or equivalently, 12 mM. The permittivity of water in our system is

$$\epsilon_0 \epsilon_r = \frac{e^2}{4\pi k_B T \lambda_B} = \frac{1}{12\pi} \cdot \frac{e^2}{k_B T \sigma}$$

Using this value of  $\epsilon_0 \epsilon_r$  ( $1/12\pi$  in our unit system) for  $\epsilon_m$ , the theoretical interpretation of our coarse-grained simulation of chain stretching yields the solvent conductivity  $\sigma_m (= \epsilon_m/\tau_{rc,m})$  equal to  $3.5 \times 10^{-5}$ , or equivalently, 0.59 S m $^{-1}$ .<sup>44</sup> This solvent conductivity agrees fairly well with the one of sodium chloride in water,<sup>45</sup> providing a self-consistent support for our theory. Here we have corrected the conductivity by dividing the value by a factor of 35. It is because the friction coefficient in eqn (4) has been set to a small value  $\zeta_i = 1.0\tau^{-1}$  in our study, which is about 35 times smaller than in water, for the purpose to accelerate the simulations. Therefore, to map diffusion-related quantities such as conductivity and relaxation time, we have to correct the obtained values by a factor of 35.

The typical RC relaxation time in experiments ranges from milliseconds to nanoseconds, depending on the ionic strength.<sup>25,42</sup> The ionic strength in our bulk solution is about  $I_s = 0.5((+1)^2 \times 10^{-4} + (-1)^2 \times 10^{-4}) = 10^{-4}$  ( $\sigma^{-3}$ ), which gives a Debye screening length equal to  $\ell_D = (4\pi\lambda_B \cdot 2I_s)^{-1/2} \approx 2.76$  nm. Using the typical value of ion diffusivity in water,  $D_i \sim 10^{-9}$  m $^2$  s $^{-1}$ ,<sup>46</sup> we expect the relaxation time in water to be a value of about  $\ell_D^2/D_i \sim 7.6$  ns. Inside the PE globule, the ions diffuse through the nanoporous structure formed by the twisted chain. The size of the nanopores is about  $\sigma$ , the diameter of the ions. Therefore, the relaxation time in PE phase is estimated by  $\sigma^2/D_i$  and the value is 58 ps. The RC time,  $\tau_{rc,p}$  and  $\tau_{rc,m}$  obtained from Fig. 3, is 20.6 ps and 1.1 ns, respectively, after multiplying by the correction

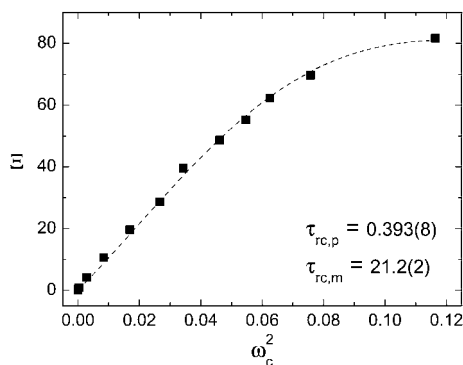


**Fig. 3**  $\Xi \equiv (|E|/E_{ad})^2 - 1$  as a function of the square of the critical frequency,  $\omega_c^2$ . The dashed curve is the result of fitting by eqn (5).

factor. These values are in fair accordance with the theoretical estimation. We remark that the RC time of highly-concentrated nanocolloid or molecule suspensions can be measured from dielectric relaxation spectroscopy or impedance spectroscopy, and the value for a single nanocolloid or molecule is inferred by an averaging theory.<sup>42</sup> Recently, cross-over frequencies of dielectrophoresis have been used to estimate the RC time of individual blood cells and nanocolloids.<sup>43,47</sup> A very recent study has demonstrated an approach to determine the RC time of short PE using fluorescent correlation spectroscopy, based upon the coil-globule transition in AC fields.<sup>25</sup>

#### D. Time variation of dipole moment and chain unfolding

The critical frequency  $\omega_c$  obtained in Sec. III.C is independent of the radius of gyration of the chain, as the Maxwell–Wagner relaxation time describes the relaxation/dissociation of ions within a Debye layer from the interface. This physical picture breakdowns when the chain begins to uncoil, such that the trivalent counter-ion no longer bridges two segments of the polyelectrolyte. Internal polarization could also develop at a different time scale. In order to understand the coupling between chain unfolding dynamics and interfacial charge relaxation/dissociation dynamics, we study here how  $p_x$  and  $D_s$  evolves in cycles ( $t/\Psi$ ) of the AC field for different values of  $\Psi$ . Value  $p_x$  is the induced dipole moment  $\vec{p}$  of the PE complex in the field direction. The PE complex, by definition, consists of the chain itself and the ions condensed inside a tube region of radius  $r_t = \lambda_B$  surrounding the chain backbone. The  $\vec{p}$  is calculated by  $\sum_i Z_i e (\vec{r}_i - \vec{r}_{cm})$  where  $i$  runs over all the particles in the PE complex and  $\vec{r}_{cm}$  is the center of mass of the chain. The results for  $|E| = 0.3$  are presented in Fig. 4.

We saw in Fig. 4(a) that  $p_x$  grows exponentially with time in every half cycle of the square-wave field and switches its sign simultaneously with the field. The growth of  $p_x$  saturates to some value if  $\Psi$  is large enough, for example,  $\Psi = 10^6 \Delta t$ . It suggests that there is a relaxation time to polarize the PE complex in an electric field. Fig. 4(b) shows that for large  $\Psi$ , the chain shrinks right after the field switches the direction, but the chain size does

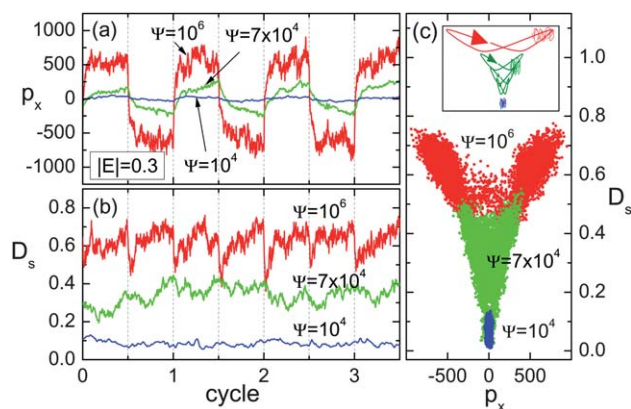


**Fig. 4** Time variation of (a)  $p_x$  and (b)  $D_s$ , against the cycle of AC field. (c) Parametric plot of  $p_x$  and  $D_s$  with time. The field strength is  $|E| = 0.3$ . The value of  $\Psi$  (in unit  $\Delta t$ ) is indicated near the associated curve and data.

not reduce down to the zero-field value. It regains its size in the corresponding DC field after  $p_x$  reaches the saturation value. On the other hand, for small  $\Psi$ , the variation of  $D_s$  is not significant. To go further, we drew the parametric plot of  $p_x$  and  $D_s$  with time in Fig. 4(c). We observed that the trajectory points travel along a butterfly curve, from the tip of one wing to the tip of the other wing, after alternating the field direction, and then wander near the region of wing tip waiting for the next switch of field direction, as sketched in the inset of the figure. The wing bottom occurs at non-zero  $p_x$ , showing that the variation of  $D_s$  falls behind the  $p_x$ . Therefore, the chain elongation is slaved to the fast dynamics of the interfacial trivalent counter-ion dissociation/relaxation time which dominates the polarization. Moreover, a beautiful shuttlecock pattern is formed when the ensemble of the data at different field frequencies is looked together in the  $p_x$ - $D_s$  plot.

### E. Polarization time and fluctuation time

To quantify the findings with our theory, we calculated the polarization time by fitting exponentially the growth of  $p_x$  in a half cycle of field with large  $\Psi$ . The mean polarization time  $\tau_p$  versus the critical period  $\Psi_c$  to unfold the chain is shown in Fig. 5(a).

We found that  $\tau_p$  depends linearly on  $\Psi_c$  with a slope equal to 0.27(1). This result interestingly connects the critical points with the polarization in the supercritical region where the chain is fully unfolded. The physics can be understood by the following simple picture. Because the chain structure is linear in the supercritical region ( $\Psi > \Psi_c$ ), the polarization time  $\tau_p$  can be estimated by the relaxation time  $R/v_d$  where  $R$  is the relaxation distance of trivalent counter-ions migrating through the chain to establish a new polarization when the applied field switches the direction and  $v_d$  is the drifting velocity equal to  $\mu_e|E|$ . In our simulations,  $\mu_e \sim 3$  for the trivalent counter-ions and  $|E| \sim 32E_{dc}^*\omega_c$  for small  $\omega_c$  according to eqn (5). The slope 0.27 yields a relaxation distance of  $R \sim 36$  (about 30% of the chain contour length), which is a reasonable value in view of the profile of charge distribution along the chain. Fig. 5(b) shows  $\tau_p$  as a function of the AC field strength  $|E|$ . One can see that the stronger the field strength, the shorter the polarization time. It is because ions and PEs are

dragged at faster speeds when the applied field is stronger. Moreover, detailed studies showed that in the region of strong field  $|E| \gg E_{dc}^*$ ,  $\tau_p$  is inversely proportional to  $|E|$ . Also, in the limit where  $|E|$  tends toward  $E_{dc}^*$ , the product of  $\tau_p^2$  and  $|E|^2 - E_{dc}^{*2}$  is a constant. The two behaviors can be deduced easily from our theory, knowing that  $\Psi_c$  and  $\tau_p$  are identical within a factor. Our simulations are in good agreement with experiments of field-induced decondensation,<sup>21</sup> in which the reciprocal of the relaxation time of decondensation exhibits a linear relation to the field strength when the field is strong, and deviates from the relation when the field is weak.

Recently, simulations done by Liu *et al.*<sup>41</sup> suggested that the intrinsic chain relaxation frequency is the upper bound of the critical AC frequency to stretch a PE chain. This bound is quite crude in light of the current result. To further verify the importance of the dissociation/condensation of the interfacial trivalent counter-ions, we calculated the autocorrelation function of  $D_s$ , defined by

$$R(t) = \frac{\langle D_s(t)D_s(0) \rangle - \langle D_s \rangle^2}{\langle D_s^2 \rangle - \langle D_s \rangle^2}$$

in different DC electric fields. The correlation time  $\tau_f$ , calculated by fitting  $R(t)$  function exponentially, represents physically the fluctuation time of chain size under the action of a DC electric field. The results have been plotted in Fig. 5(b) as a function of the field strength  $E_{dc}$  at the same scale. We found that  $\tau_f$  is a constant when  $E_{dc} < E_{dc}^*$ . A large jump occurs at  $E_{dc} = E_{dc}^*$  and then,  $\tau_f$  decreases inversely with increasing  $E_{dc}$ . A striking finding is that  $\tau_f$  is basically coincident with  $\tau_p$  in the region  $E_{dc} > E_{dc}^*$ . We know that the PE chain is in a dynamic equilibrium with the ions surrounding it. The dissociation or condensation of a counterion away or onto the chain will locally break the chain stability and cause the fluctuation of the chain size. The coincidence between these characteristic times shows the importance of the ion fluctuations on chain unfolding. The critical frequency to stretch a chain in a square-wave AC field is mainly determined by the dissociation/relaxation of the condensed interfacial trivalent counter-ions, which takes the value of the fluctuation time of chain size in the counterpart DC electric field.

## IV. Summary

We have revealed the key conditions to unfold collapsed PE chains in square-wave AC electric fields: the field strength must be larger than the critical DC field to stretch the chain and the frequency is smaller than the inverse of the counterion dissociation/relaxation time under a quasi-DC field. Moreover, when both conditions are satisfied, there is a strong correlation between the critical field strength and the field frequency. A simple scaling theory, based upon Maxwell–Wagner dielectric theory, can quantitatively capture this critical field-frequency correlation for PE unfolding in AC fields.

This material is based upon work supported by the National Science Council, the Republic of China, under Grant No. NSC 97-2112-M-007-007-MY3. Computing resources are supported by the National Center for High-performance Computing. HCC is supported by DTRA (HDTRA1-08-C-0016).

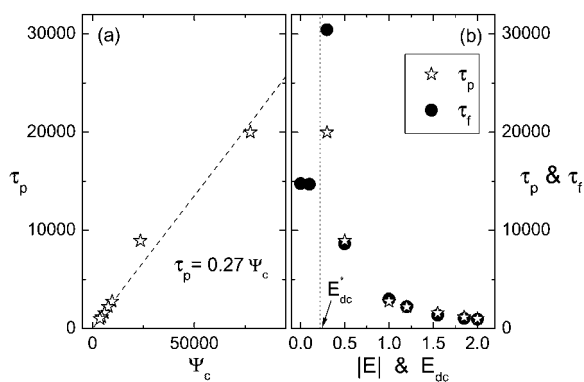


**Fig. 5** (a) Polarization time  $\tau_p$  vs. critical period  $\Psi_c$ , and (b)  $\tau_p$  vs. field strength  $|E|$ . In panel (b), fluctuation time  $\tau_f$  is also plotted as a function of  $E_{dc}$  at the same scale. The values of  $\tau_p$ ,  $\tau_f$  and  $\Psi_c$  are reported in unit  $\Delta t$ .

## References

- 1 J. Shendure, R. D. Mitra, C. Varma and G. M. Church, *Nat. Rev. Genet.*, 2004, **5**, 335.
- 2 E. Y. Chan, *Mutat. Res., Fundam. Mol. Mech. Mutagen.*, 2005, **573**, 13.
- 3 P. K. Gupta, *Trends Biotechnol.*, 2008, **26**, 602.
- 4 R. Treffer and V. Deckert, *Curr. Opin. Biotechnol.*, 2010, **21**, 4.
- 5 F. Sanger, S. Nicklen and A. R. Coulson, *Proc. Natl. Acad. Sci. U. S. A.*, 1977, **74**, 5463.
- 6 S. B. Smith, Y. Cui and C. Bustamante, *Science*, 1996, **271**, 795.
- 7 T. T. Perkins, D. E. Smith, R. G. Larson and S. Chu, *Science*, 1995, **268**, 83.
- 8 M. Washizu and O. Kurosawa, *IEEE Trans. Ind. Appl.*, 1990, **26**, 1165.
- 9 M. Washizu, O. Kurosawa, I. Arai, S. Suzuki and N. Shimamoto, *IEEE Trans. Ind. Appl.*, 1995, **31**, 447.
- 10 N. Kaji, M. Ueda and Y. Baba, *Biophys. J.*, 2002, **82**, 335.
- 11 N. Kaji, M. Ueda and Y. Baba, *Appl. Phys. Lett.*, 2003, **83**, 3413.
- 12 S. Ferree and H. W. Blanch, *Biophys. J.*, 2003, **85**, 2539.
- 13 J. O. Tegenfeldt, O. Bakajin, C.-F. Chou, S. S. Chan, R. Austin, W. Fann, L. Liou, E. Chan, T. Duke and E. C. Cox, *Phys. Rev. Lett.*, 2001, **86**, 1378.
- 14 A. Bensimon, A. J. Simon, A. Chiffaudel, V. V. Crouquette, F. Heslot and D. Bensimon, *Science*, 1994, **265**, 2096.
- 15 S. B. Smith, L. Finzi and C. Bustamante, *Science*, 1992, **258**, 1122.
- 16 M. P. Hughes, *Nanotechnology*, 2000, **11**, 124.
- 17 I.-F. Cheng, S. Senapati, S. Cheng, H.-C. Chang and H.-C. Chang, *Lab Chip*, 2010, **10**, 828.
- 18 H. Cottet and J.-L. Viovy, *Electrophoresis*, 1998, **19**, 2151.
- 19 J.-L. Viovy, *Rev. Mod. Phys.*, 2000, **72**, 813.
- 20 S. B. Smith, P. K. Aldridge and J. B. Callis, *Science*, 1989, **243**, 203.
- 21 D. Porschke, *Annu. Rev. Phys. Chem.*, 1985, **36**, 159.
- 22 H.-C. Chang, *AIChE J.*, 2007, **53**, 2486.
- 23 M. Washizu, *Inst. Phys. Conf. Ser.*, 2004, **178**, 89.
- 24 V. R. Dukkipati and S. W. Pang, *Appl. Phys. Lett.*, 2007, **90**, 083901.
- 25 S. Wang, H.-C. Chang and Y. Zhu, *Macromolecules*, 2010, **43**, 7402.
- 26 V. A. Bloomfield, *Curr. Opin. Struct. Biol.*, 1996, **6**, 334.
- 27 P.-Y. Hsiao and E. Luijten, *Phys. Rev. Lett.*, 2006, **97**, 148301.
- 28 D. Porschke, *Biopolymers*, 1985, **24**, 1981.
- 29 R. R. Netz, *Phys. Rev. Lett.*, 2003, **90**, 128104.
- 30 R. R. Netz, *J. Phys. Chem. B*, 2003, **107**, 8208.
- 31 P.-Y. Hsiao and K.-M. Wu, *J. Phys. Chem. B*, 2008, **112**, 13177.
- 32 Y.-F. Wei and P.-Y. Hsiao, *Biomicrofluidics*, 2009, **3**, 022410.
- 33 N. Chetwani, C. A. Cassou, D. B. Go and H.-C. Chang, *J. Am. Soc. Mass Spectrom.*, DOI: 10.1016/j.jasms.2010.06.023.
- 34 R. W. Hockney, and J. Y. Eastwood, *Computer Simulation Using Particles*, Taylor & Francis, 1988.
- 35 P.-Y. Hsiao, *J. Chem. Phys.*, 2006, **124**, 044904.
- 36 P.-Y. Hsiao, *Macromolecules*, 2006, **39**, 7125.
- 37 The simulations were run using modified LAMMPS package (<http://lammmps.sandia.gov/>).
- 38 M. Tanaka and A. Y. Grosberg, *Eur. Phys. J. E: Soft Matter Biol. Phys.*, 2002, **7**, 371; M. Tanaka, *Phys. Rev. E: Stat., Nonlinear, Soft Matter Phys.*, 2003, **68**, 061501.
- 39 D. Long, J.-L. Viovy and A. Ajdari, *Phys. Rev. Lett.*, 1996, **76**, 3858.
- 40 K. Grass and C. Holm, *Soft Matter*, 2009, **5**, 2079.
- 41 H. Liu, Y. Zhu and E. Maginn, *Macromolecules*, 2010, **43**, 4805.
- 42 H.-C. Chang, and L. Y. Yeo, *Electrokinetically Driven Microfluidics and Nanofluidics*, Cambridge University Press, 2010.
- 43 S. Basuray and H.-C. Chang, *Phys. Rev. E: Stat., Nonlinear, Soft Matter Phys.*, 2007, **75**, 060501.
- 44 In our system, the unit of conductivity is  $e^2/(k_B T \sigma)$  which corresponds to 17 200 siemens per meter ( $S m^{-1}$ ).
- 45 Y. C. Wu and P. A. Berezansky, *J. Res. Natl. Inst. Stand. Technol.*, 1995, **100**, 521.
- 46 A. N. Campbell and B. G. Oliver, *Can. J. Chem.*, 1969, **47**, 2681.
- 47 J. E. Gordon, Z. Gagnon and H.-C. Chang, *Biomicrofluidics*, 2007, **1**, 044102.